Carbonation of loaded RC elements made of different concrete types

Wang, Xiao-Hui; Val, Dimitri V.; Zheng, Li; Jones, M. Roderick

Published in:
Construction and Building Materials

DOI:
10.1016/j.conbuildmat.2020.118259

Publication date:
2020

Document Version
Peer reviewed version

Carbonation of loaded RC elements made of different concrete types: accelerated testing and future predictions

Xiao-Hui Wang [a,*], Dimitri V. Val [b], Li Zheng [c], M. Roderick Jones [c]

[a] College of Ocean Science and Engineering, Shanghai Maritime University, Shanghai 201306, China

[b] Institute for Infrastructure & Environment, Heriot-Watt University, Edinburgh, UK

[c] Concrete Technology Unit, Division of Civil Engineering, University of Dundee, Dundee, UK

Abstract

Carbonation of concrete can lead to corrosion of reinforcing bars. By this reason its prediction is very important, in particular for durability design, e.g. determining the minimum thickness of the concrete cover. Although carbonation of concrete in reinforced concrete (RC) structures is influenced by applied loading, limited research has been carried out in this area, especially for 'green/low carbon' concretes, i.e. mixes containing supplementary cementitious materials such as fly ash (FA) and ground granulated blast-furnace slag (GGBS). This paper reports the influence of structural loading on carbonation of three types of concrete: Portland cement (PC), PC with 30% of FA and PC with 50% of GGBS, with two water/ binder (w/b) ratios (0.40 and 0.55). Test specimens made with these concretes, i.e. 100-mm cubes (unloaded) and RC beams (loaded), were subject to accelerated carbonation (CO_2 content of 4%) for a duration of up to 240 days. Results of the tests are presented in this paper along with their analysis, in particular, the evaluation of the carbonation coefficients. The results clearly show a significant influence of loading on carbonation rate. Based on the test results, the estimated effects of loading on carbonation after 50 and 100 years exposure have been calculated. These estimates indicate that the current durability requirements in the Eurocodes may not be adequate for preventing the initiation of carbonation-induced corrosion in tensile zones of RC elements during their design working life.

Keywords: accelerated carbonation; fly ash (FA); granulated blast-furnace slag (GGBS); load-induced cracks; carbonation rate; carbonation depth prediction.

* Corresponding author. E-mail: w_xiaoh@163.com

1. Introduction

To reduce the anthropogenic emissions of greenhouse gases — most notably carbon dioxide (CO_2) — associated with the concrete industry, Portland cement (PC) is often replaced with supplementary cementitious materials, mostly industrial by-products such as fly ash (FA), blast furnace slag (GGBS) and silica fume [1]. Concretes containing such materials are often referred to as 'green' concretes [2].

Concrete also reabsorbs CO_2 during its service life that partially offsets the emissions associated with its production (e.g. [3]). This occurs due to carbonation, a natural process in which CO_2 reacts with the alkaline cement hydration products, in particular with calcium hydroxide, $Ca(OH)_2$, that reduces the pore fluid alkalinity of concrete. Thus, when the carbonation front reaches reinforcing steel embedded in concrete, it can remove the passivity of carbon steel and lead to its corrosion and subsequent damage to the reinforced concrete (RC) element [4]. The propagation of corrosion in RC elements and damage caused by it are mainly of interest for the assessment of existing RC structures, their maintenance planning and life-cycle analysis (e.g. [5-8]). Durability design is based on prevention, or more exactly reducing the risk, of premature corrosion initiation and requires a minimum concrete cover to be specified in combination with concrete grade and maximum water/ binder (w/b) ratio (e.g. [9]). To determine the durability specifications for RC structures exposed to carbonation, the resistance of concrete to the latter needs to be known.

The carbonation resistance of different concrete mixes has been extensively studied (e.g. [10-29]). In particular, based on systematic analysis of data from 213 and 227 studies for FA [26] and GGBS concretes [27], respectively, it was concluded that the carbonation rates of both FA and GGBS concretes are higher than of PC concretes with the same water/ binder (w/b) ratio (although this may not be the case for equal strength mixes). However, in the context of the durability requirements from all concretes containing FA or GGBS, only CEM IV/B concrete, which has a high percentage of FA (36% to 55%), is treated differently from PC concretes when the prevention of carbonation-induced corrosion is of concern [9].

All above mentioned studies have dealt with carbonation of unloaded concrete, i.e. concrete elements which are not subject to structural loading and, subsequently, load-imposed stresses. However, RC elements in real structures are under loading but only a few studies have investigated carbonation of concrete in a stressed state [30-34]. These studies indicated a significant influence of stresses, especially tensile stresses, on the rate of carbonation. Tensile stresses in concrete also lead to cracking and its effects on carbonation have been reported in [35-36]. In particular, accelerated tests (with a CO_2 concentration of 50%) showed that CO_2 penetration along a crack path depended on the crack width – CO_2 diffused freely through cracks of width of 60μm or wider, while there was no carbonation penetration perpendicular to the crack wall for crack widths of 9μm or smaller [35]. Recently, Dang et al. [36] reported the initiation and propagation of corrosion in mortar specimens pre-cracked by mechanical loading (crack widths ranged from 27μm to 395μm) and carbonated in accelerated conditions (CO_2 50%) for 15-23 weeks. It was observed that initiation and propagation of corrosion was accelerated by load-induced cover cracking.

Even fewer studies have addressed the influence of loading and cracking on carbonation of 'green' concretes [33, 34]. Wang et al. [33] conducted tests to examine the effects of compressive and tensile stresses and high exposure temperature on the carbonation resistance of PC and FA concretes. The test results showed that the carbonation resistance of both types of concrete decreased with an increase in the tensile stress level. As compressive stress was raised, the carbonation resistance initially increased (for stresses up to about 30% of the concrete compressive strength, f_c') and then started to decrease; it became equal the carbonation resistance of unloaded concrete at the stress level of about $0.5 f_c'$ before dropping below it. In Wang et al. [34], the authors presented results of the first stage of an experimental investigation into the influence of loading and associated concrete cracking on carbonation of RC elements made of PC and 'green' concretes containing FA and GGBS. In these tests, six concrete mixes with two w/b ratios (0.40 and 0.55) and different proportions of PC, FA and GGBS were prepared. The mixes were used to cast 24 RC beams (100×120×900mm) and a number of 100-mm concrete cubes. The RC beam specimens were loaded in four-point bending to

produce cracks of two nominal widths – 0.1 mm and 0.3 mm. After that, both RC beam specimens (loaded) and concrete cubes (unloaded) were placed into a carbonation chamber. The carbonation depths measured in the concrete cubes and twelve RC beams after 120 days of accelerated carbonation (4% CO_2 concentration) were reported.

The present paper reports results of the second stage of the experiment, in which the carbonation depths were measured in the remaining concrete cubes and twelve RC beams after 240 days of accelerated carbonation. A brief description of the experimental setup is also provided. After that, results of the whole experiment are summarised and the carbonation coefficients for the unloaded and loaded (in tension) concretes are evaluated. The results clearly show a major influence of loading on the carbonation rates of the concretes, especially of the 'green' concretes. Based on the test results, the carbonation depths in RC structures made of similar concretes after 50 and 100 years in service under natural conditions are estimated. These estimates indicate that the current durability requirements in the Eurocodes [9] are inadequate for preventing the initiation of carbonation-induced corrosion in tensile zones of RC elements made of the 'green' concretes during their design working life, especially in the light of a continuous increase of the CO_2 atmospheric concentration.

2. Experimental Programme

This section provides a brief description of the experimental program. More detailed information about it can be found in Wang et al. [34].

Six concrete mixes including PC (i.e. Portland cement) (CEM I52.5 N), FA (i.e. fly ash) (30%) and GGBS (i.e. ground granulated blast-furnace slag) (50%) with two w/b ratios – 0.40 and 0.55, were used in the experiments. From each of these mixes, a number of 100-mm concrete cubes and four RC beams with a rectangular cross section of 100×120 mm and length 900 mm (see Fig.1a) were made. After curing, all specimens (i.e. both beams and cubes) intended for accelerated carbonation were kept for about three months. Then, the beam specimens were statically loaded in four-point bending. The level of the applied load was controlled to ensure that the maximum width of cracks in the tensile zone of the beams due to bending was either nominal 0.1 mm or 0.3 mm. After the beams

had been loaded and cracked, they were placed in pairs and the actual dimensions of the beams and cracks in each beam were measured and recorded, see Table 1 (only for the beams that were kept in the carbonation chamber for 240 days, for the rest of the beams see [34]).

The cubes and the beam pairs were kept in the carbonation chamber for 120 days (stage one, see [34]) and 240 days (stage two, see Fig.1b). Then, they had been removed from the carbonation chamber and were cut into two halves longitudinally. The split/sawed surfaces were sprayed with a phenolphthalein solution and carbonation depths were then measured at 10 mm intervals.

3. Test Results and Discussion

3.1 Cracks in RC beam specimens

The types of cracks observed in the beam specimens from stage two are similar to those in beam specimens from stage one [34], i.e. 1) flexural cracks in the tensile zone; (2) shear cracks in the zones with shear stresses (i.e. zones within the loaded part of the beams outside the 200-mm central part); and (3) hairline drying shrinkage cracks at the top of the beams (i.e. near the casting surface). For each beam specimen subjected to 240-day accelerated carbonation (stage two), the maximum crack width at the bottom of the specimen before it was placed in the carbonation chamber is given in Table 1. It is important to note that loads in the beam specimen pairs were not checked and controlled while the specimens were in the carbonation chamber. Hence, the loads acting on the beam specimens decreased over the duration of the test due to creep and cracks could partially or fully close over that time. This also means that the initial differences in internal stresses between the beam specimens with nominal 0.1mm and 0.3mm crack widths also mainly disappeared with time. Further information on the crack patterns in the beam specimens can be found in [34].

3.2 Comparison of carbonation depths in unloaded concrete cubes and loaded beam specimens

The carbonation depths in unloaded concrete cubes are summarised in Table 2. The depths are averages of the measurements made in two parts of a split cube. It can be seen from Table 2 that the 040PC cubes were practically uncarbonated, while the 055FA ones were nearly fully carbonated.

The average carbonation depths within the pure bending zone of the beam specimens have been

calculated by excluding the influence of visible cracks, i.e. the carbonation depths measured within the vicinity of visible cracks have not been taken into account in these calculations, and are also shown in Table 2. The average depths given in Table 2 are averaged over two halves of each beam. The values of the maximum carbonation depths at the top and bottom of the beam specimens along their whole lengths are also presented. The 055FA beams were fully carbonated so that the values of the carbonation propagation, which can be expected in this loaded concrete over 240 days, cannot be accurately determined. It can only be stated that the carbonation depth should be equal or greater than half of the dimension of the beam depth, i.e. 60 mm. Parts of the 040FA and 055GGBS beams were also fully carbonated that did not allow to provide specific values of the maximum carbonation depth for these beams.

For three concrete types with the same w/b ratio, i.e. PC, FA or GGBS, due to the different CO_2 binding capacity and porosity (or, more exactly, interconnected porosity) (e.g. [17]), the carbonation depths in unloaded concrete cubes are quite different. For concrete cubes with 0.40 w/b ratio, the 040PC concrete demonstrated the highest carbonation resistance although its porosity was slightly higher than that of the 040GGBS concrete (see Table 3), while the 040FA concrete had the highest porosity and the lowest carbonation resistance (the average carbonation depth in its cubes was 25.9mm) . For concrete cubes with 0.55 w/b ratio, the 055FA concrete had the highest porosity (see Table 3) and the cubes made of it were nearly totally carbonated after 240-day accelerated carbonation, see Table 2.

Now, the carbonation depths in the unloaded cubes and the loaded beams specimens are compared to examine the influence of loading on the carbonation depth and resistance. The top part of the loaded beams was in compression, while their bottom part – in tension.

There is no conclusive evidence regarding the influence of compressive stresses. Only for the 055PC concrete, the average carbonation depth at the top of the beams was smaller than that in the cube (i.e. the average values 21.8 mm and 19.6 mm in the beams vs. the average value 28.4 mm in the cube, see Table 2); for the FA concretes, they were slightly larger (31.3 mm vs. 25.2 mm for

040FA and ≥50 mm vs. 47.4 mm for 055FA); while for the GGBS concretes, they were significantly larger (20.1 mm, 19.5 mm and 19.8 mm vs. 10.3 mm for 040GGBS, and 39.6 mm and 47.5 mm vs. 23.0 mm for 055GGBS). It was observed in [33] that for PC and FA concretes an increase in compressive stresses initially led to an increase in the carbonation resistance (for stresses up to about 0.5 of the compressive concrete strength f_c') and then the latter started to decrease due to damage caused by the stresses to the concrete microstructure. It is worth to mention that the CO_2 concentration in those tests was 20±3% and the carbonation duration 7 and 14 days [33]. In the present tests, the effect of compressive stresses on the carbonation resistance depended mainly on the concrete composition rather than on the stress level since in all beam specimens the level of compressive stresses over the duration of the test was approximately the same and lower than 0.5 f_c'. In the 055PC concrete, similar to the results in [33], compressive stresses led to an increase in the carbonation resistance. In the FA concretes, compressive stresses led to a slight decrease of the carbonation resistance; this result is not completely different from those [33], in which the decrease in the carbonation resistance of concrete with 30% FA occurred faster than that of PC concrete after the stress level exceeded 0.3 f_c'. The most significant negative effect of compressive stresses on the carbonation resistance was observed for the GGBS concretes (such concretes were not tested in [33]). This can be attributed to damage to the concrete microstructure, more exactly, to blocking between the concrete pores and, subsequently, an increase in the interconnected porosity. Further evidence supporting this hypothesis will be discussed later. In terms of the carbonation resistance under compressive stresses, the concretes tested in this study are ranked in the following order (from lowest to highest): 055FA, 055GGBS, 040FA, 055PC, 040GGBS and 040PC.

Negative influence of tensile stresses on the carbonation resistance (i.e. its decrease) has been demonstrated by all concretes that were tested, except of 040PC (for this concrete practically no signs of carbonation, both in the cube and the beams, were observed). The average carbonation depths at the bottom of the beams were significantly larger than those at the bottom of the cubes made from the same type of concrete (see Table 2). This is in agreement with previously reported experimental

results [30-34]. Regarding the influence of the initial level of applied load, i.e. comparing the average carbonation depths at the bottom of the beam specimens with 0.1mm and 0.3mm nominal initially-induced flexural cracks, it can be seen that for all concrete types for which relevant data are available (055PC, 040GGBS and 055GGBS), the depths in the specimens with the 0.3mm nominal cracks are slightly larger. Since the level of load applied to all beams (i.e. with both initial crack widths) during the 240-day accelerated carbonation was more or less the same, this difference can be explained by damage introduced to the concrete microstructure of the beams when they first loaded to produce the cracks. The initial damage was obviously larger in the beams with 0.3mm nominal wide cracks. The most significant increase in the average carbonation depths compared to the unloaded cubes occurred in the GGBS concretes. This is another indication that the damage led to an increase in the interconnected porosity of the concretes, especially of the GGBS concretes. Based on the average bottom carbonation depths in the beam specimens (see Table 2), the concretes can be ranked in the following order in terms of their carbonation resistance under tensile stresses (from lowest to highest): 055FA, 055GGBS, 040FA, 055PC, 040GGBS and 040PC, which is exactly the same as under compressive stresses.

3.3 Comparison of carbonation profiles of typical loaded beams with different concrete types and w/b ratios

For loaded beam specimens with the w/b ratio of 0.40, there is no carbonation in beams 040PC. Comparison of carbonation profiles of typical loaded beams made of 040FA and 040GGBS is shown in Fig.2. It can be seen from Fig.2a that in the cross-section with inclined shear cracks the concrete was totally carbonated. In the beam zone with vertical cracks, comparatively deeper carbonation depth is observed at or nearby crack locations as well as the stirrups locations (see Fig.2). For loaded beam specimens with the w/b ratio of 0.55, comparison of carbonation profiles of typical loaded beams made of 055PC, 055FA and 055GGBS is shown in Fig.3. Among the three types of concrete, the 055PC beam demonstrated the lowest carbonation depth, while the 055FA beam was totally carbonated (see Fig.3b) and most part of the 055GGBS beam was carbonated through the whole beam

height (see Fig.3c).

For the same concrete type with different w/b ratios, deeper carbonation depth was always observed in concrete with lager w/b ratio (see Table 2 and Figs.2-3) showing that the increase in the w/b ratio resulted in lager concrete porosity and decreased concrete resistance to carbonation.

The results for the FA concretes demonstrating their lower carbonation resistance compared to that of PC and GGBS concretes are similar to most of the previous studies [26, 27]. Regarding the GGBS and PC concretes, it is often suggested that the carbonation resistance of GGBS concretes is lower than that of PC concrete with a similar w/b ratio, especially when the GGBS content is greater than 20% [27]. For the loaded beams, the carbonation resistance of GGBS concretes is lower than that of PC concrete, as shown in Figs.2-3; while for the unloaded cubes with the w/b ratio of 0.55, due to the higher porosity of the 055PC concrete compared to that of 055GGBS (see Table 3), larger carbonation depth is observed in 055PC, see Table 2.

3.4 Comparison of results after 120 and 240 days of accelerated carbonation

First of all, it is important to note that the rankings of the carbonation resistance of the unloaded and loaded concretes based on the accelerated test results after 120 days (stage one) [34] and 240 days (stage two) are exactly the same. Since different specimens, although made of the same concretes, were tested at the stages one and two, this provides evidence of the consistency of the test results.

In more detail, regarding the effect of compressive stresses on the carbonation resistance, there are some differences between the stage one and stage two results. At the stage one, the average carbonation depths at the top of the beams were smaller than those in the corresponding cubes for the following concretes: 055PC, 040FA, 055FA and 040GGBS, and only larger for 055GGBS (no carbonation in 040PC) [34]. At the first glance, these results look significantly different from the stage two results, in which the smaller average carbonation depth was observed only at the top of the 055PC beam (see Table 2 and discussion in Section 3.2). However, a closer consideration of the results shows that, for the 040FA and 055FA concretes, the differences between the average carbonation depths at the top of the beams and the cubes were small at both stages – at the stage one they were slightly

smaller in the beams; while at the stage two – in the cubes. This could occur, for example, due to constant reduction of the magnitude of compressive stresses in the beam specimens over time. For the 040GGBS concrete, only one beam specimen (040GGBS03) was tested at the stage one and the difference between the average carbonation depths at the top of the beam and the cube was very small – 10.6 mm in the beam vs. 11.6 mm in the cube (see **Table 1A in** Appendix A). At the stage two, three beam specimens of the 040GGBS concrete were tested; thus, the result that compressive stresses in this concrete led to an increase in the average carbonation depth was much more reliable. Moreover, the argument about the reduction of compressive stresses over time made for the 040FA and 055FA concretes is also relevant for this case. Noticeable differences between the average carbonation depths at the top of the beams and the cubes were observed at both stages only for the 055PC and 055GGBS concretes and these results are consistent – for 055PC the depths in the beams were smaller, while for 055GGBS – larger.

Results related to the influence of tensile stresses on the carbonation resistance are fully consistent between the two stages. For all concretes (except of 040PC, for which no carbonation was observed) at both stages, tensile stresses led to a decrease in the carbonation resistance, i.e. larger average carbonation depths at the bottom of the beam specimens compared to those in the cubes. The effect of the level of initially applied loading on the carbonation resistance (i.e. beam specimens with 0.1mm nominal initially-induced cracks vs. those with 0.3mm nominal cracks) is inconclusive for the stage one results. For two concretes – 040FA and 055GGBS, the average carbonation depths at the bottom of the beam specimens with 0.3mm nominal wide cracks were larger than those in the beams with 0.1mm nominal wide cracks; for the 055PC and 055FA concretes the opposite was observed; no relevant data were available for the 040PC (no carbonation) and 040GGBS (only one beam specimen was tested) concretes [34]. Since at the stage two, the average carbonation depths in the beam specimens with 0.1mm and 0.3mm nominal wide cracks made of the same concrete do not differ significantly, in the following analysis the data for the beam specimens from the same concrete but with different nominal crack widths will be combined and represented by a single average value for

each stage, i.e. one value of the average carbonation depth after 120 days and another value after 240 days for all beam specimens from the same concrete.

The average carbonation depths after 120 and 240 days at the bottom of the unloaded cubes and the loaded beam specimens are shown by markers in Figs.4a and 4b, respectively. The propagation of the carbonation front into concrete is usually modelled by Fick's first law of diffusion so that the carbonation depth is directly proportional to the square root of the time of carbonation exposure (e.g. [37]). This also means that the carbonation rate decreases over time. The resulting carbonation depths (markers in Fig.4) mainly follow this pattern. One noticeable exception is the results for the 040GGBS cubes (i.e. unloaded) – see Fig.4a, where the average carbonation depth after 240 days is smaller than that after 120 days. It is important to note that these results are based on the carbonation depth measurements in just two cubes for each of the concretes – one after 120 days and the other one after 240 days. Thus, the most probable causes of these inconsistencies are some differences in the cubes' compaction, curing, exposure, etc. The results for the loaded concretes (Fig.4b) are more consistent that is not surprising since almost every point shown in the figure is based on the carbonation depth measurements in at least two beam specimens.

4. Carbonation Predictions Based on Test Results

As noted previously, the most common simple model for predicting the carbonation depth, x_c, in concrete at time t can be expressed as (e.g. [17, 21, 38])

$$x_c(t) = A\sqrt{t} \tag{1}$$

where A is the carbonation coefficient, t time (years) and $x_c(t)$ the carbonation depth (mm). Using the values of the carbonation depths from the accelerated tests (i.e. the points shown by markers in Fig.4) values of A for all tested concretes (except of 040PC, which did not experience any noticeable carbonation) in unloaded and loaded (tension) states have been estimated by linear regression analysis based on a liner relationship between x_c and $\sqrt{t}$. These values of A are presented in Table 4, while the corresponding predictions of the carbonation depth using Eq. (1) are shown by lines in Fig.4. It is worth to note that in all cases, except of two, the values of the coefficient of determination R^2 in the

linear regression analyses were greater than 0.9. These two exceptions – unloaded 055FA and 040GGBS concretes, were discussed in the previous section; for them the R^2-values were 0.87 and 0.73, respectively.

Table 4 also presents the ratio between the values of A for loaded and unloaded concretes of the same type, A_l/A_u. As can be seen, the largest ratios, i.e. the largest increases in the carbonation rate due tensile stresses, are for the GGBS concretes. The ratios for the FA concretes are similar to that for the 055PC concrete; however, the carbonation coefficients for the FA concretes are higher than those for 055PC, especially for 055FA. A more than two times increase in the carbonation coefficient for the GGBS concretes after they were submitted to tensile stresses can be explained by damage to the concrete microstructure, which led to a major increase in the interconnected porosity of the concretes. In other words, before loading was applied, a large proportion of pores in the concretes had been blocked but damage caused by the loading significantly increased the pore connectivity. Of course, this hypothesis needs further experimental checking but the tests performed in the present study provided indirect evidence in its support as was previously discussed in the paper.

Values of the carbonation coefficient based on accelerated carbonation tests can be used to estimate the carbonation depths in real RC structures made from similar concrete as [17, 21]

$$x_c(t) = A\sqrt{\frac{C_c^r}{C_c^t}}\sqrt{t} \tag{2}$$

where C_c^t and C_c^r are the CO_2 concentrations in the test and the atmosphere, respectively. Of course, other ambient parameters such as temperature and RH may differ from those in the test that will also affect the carbonation process in real RC structures and can be taken into account as well. However, in order to keep the following discussion as simple as possible only the influence of the most important parameter for concrete carbonation, namely the CO_2 concentration (e.g. [39]), is considered herein.

The CO_2 concentration in the tests used to obtain the values of A in Table 4 was 4%, the current atmospheric CO_2 concentration is about 407 ppm [40], hence, $\sqrt{C_c^r/C_c^t} \cong 0.10$. The design working

life of structures is typically 50 or 100 years [41]. The carbonation depths in real RC structures made from the concretes tested in this study are then calculated for 50 and 100 years and the results are presented in Tables 5 and 6, respectively. The tables also show the minimum requirements regarding the concrete cover for RC structures exposed to carbonation (i.e. exposure classes XC); the minimum thicknesses of the concrete cover include an allowance in design for deviation, Δc_{dev}, which is taken equal to 10 mm. As can be seen, the carbonation depths in the 040FA, 055FA and 055GGBS concretes under loading (i.e. subject to tensile stresses) after both 50 and 100 years exceed the corresponding required thicknesses of the concrete cover. This means that the current Eurocode durability requirements for RC structures made from concretes with FA and GGBS may be inadequate for preventing carbonation-induced corrosion.

The carbonation depths in Tables 5 and 6 have been calculated based on the average atmospheric concentration of CO_2, while there is evidence that in urban or industrial areas this concentration can be significantly higher (e.g. [42]). Based on available data, it was suggested that the CO_2 concentration in urban areas was expected to be 1.15 times higher than its average value [43]. Thus, it is expected that in urban areas the carbonations depths are about 7% larger than the values in Tables 5 and 6. Moreover, due to human activities, the CO_2 atmospheric concentration constantly increases over time, with a current rate of about 2 ppm per year [42]. According to the IPCC, the CO_2 atmospheric concentration in 2100 will be between 540 ppm and 970 ppm depending on an emissions scenario [44]. For example, assuming that the average CO_2 atmospheric concentration in the next 100 years is 500 ppm, then the carbonation depths in the concretes in an urban environment over this period of time will increase by 20% compared to the values in Table 6. This means that these depths will exceed the required thicknesses in the 040FA, 055FA and 055GGBS concretes for all considered exposure classes and in the 055PC for the exposure classes XC2/XC3; moreover, in the 055FA it will occur in both loaded and unloaded states.

It is worth to note that the above estimations of the long-term carbonation propagation are an approximation. Eq. (2) used for this purpose does not account for the actual environmental conditions

(e.g. temperature, relative humidity), which may have a noticeable effect on the carbonation propagation in a particular RC structure. Moreover, it does not take into account the influences of long-term chemical processes in concrete except of the carbonation itself. Currently, there is not enough data to consider these influences in a sufficiently accurate and reliable way, especially for the "green" concretes subject to load-induced stresses. Thus, to obtain more accurate predictions of the long-term carbonation propagation, more information needs to be collected on the carbonation performance of various concretes in real RC structures over a sufficiently long period of time (i.e. dozens of years). However, before such information will become available in the future the durability design of RC structures still needs to be carried out. For that reason, accelerated carbonation tests in combination with simple models, like the one used in this study, are usually employed at present to predict the carbonation performance of various concretes.

5. Conclusions

Accelerated carbonation in unloaded and loaded concrete specimens made from PC, FA and GGBS concretes with two w/b ratios – 0.40 and 0.55, was experimentally studied. Results of the tests demonstrated that the concrete composition, i.e. w/b ratio and content of FA and GGBS, had a major influence on the carbonation resistance of the concretes. As expected, concretes of the same type with the larger w/b ratio of 0.55 had a lower carbonation resistance than those with the w/b ratio of 0.40. In both unloaded and loaded states, the 040PC concrete had the highest carbonation resistance and the 055FA concrete – the lowest. The results also showed a major influence of loading, especially tensile stresses, on the carbonation resistance of the concretes. This resistance significantly decreased in bottom parts of the tested beam specimens that were in tension. The largest decrease was observed in the specimens made from the GGBS concretes. This decrease can be explained by an increase in the interconnected porosity of the concretes due to damage caused by applied loading. The tests also demonstrated the effect of visible load-induced cracks, both flexural and shear, on concrete carbonation.

Using the test data and the most common model of concrete carbonation based on Fick's first

law of diffusion, the carbonation depths in real RC elements made of concretes similar to those in the tests were estimated for typical design working lives of 50 and 100 years. It was observed that these carbonation depths in loaded specimens made of the 040FA, 055FA and 055GGBS concretes exceeded the minimum thicknesses of the concrete cover currently required by the Eurocode 2. This indicates that the current durability requirements in the Eurocodes [9] may be inadequate for preventing carbonation-induced corrosion in RC elements made from 'green' concretes, which contain FA and GGBS. This is further aggravated by the fact that the CO_2 atmospheric concentration constantly increases due to human activities.

Acknowledgments

This research was supported by the HORIZON 2020 Marie Skłodowska-Curie Research Fellowship Programme H2020 - 658475, titled: "Climate-resilient pathways for the development of concrete infrastructure: adaptation, mitigation and sustainability (ClimatCon)".

References

[1] C. Meyer, The greening of the concrete industry, Cem. Concr. Compos. 31(8) (2009) 601-605.

[2] J. S. Damtoft, J. Lukasik, D. Herfort, D. Sorrentino, E.M. Gartner, Sustainable development and climate change initiatives, Cem. Concr. Res. 8 (2008) 115-127.

[3] L. Haselbach, Potential for carbon dioxide absorption in concrete, J. Environ. Eng. ASCE 135(6) (2009) 465-472.

[4] A. Bentur, N. Berke, S. Diamond, Steel corrosion in concrete: fundamentals and civil engineering practice, London: E&FN Spon Press, 1998.

[5] C. Q. Li, Life cycle modelling of corrosion affected concrete structures – propagation, J. Struct. Eng., ASCE 129(6) (2003) 753-761.

[6] C. Q. Li, R. E. Melchers, Time-dependent risk assessment of structural deterioration caused by reinforcement corrosion, ACI Struct J. 102(5) (2005) 754-762.

[7] F. Biondini, F. Bontempi, D. M. Frangopol, P. G. Malerba, Probabilistic service life assessment and maintenance planning of concrete structures, J. Struct. Eng., ASCE 132(5) (2006) 810-825.

[8] P. F. Marques, C. Chastre, Â. Nunes, Carbonation service life modelling of RC structures for concrete with Portland and blended cements, Cem. Concr. Compos. 37 (2013) 171-184.

[9] EN 1992-1-1. Eurocode 2, Design of Concrete Structures. Part 1–1: general rules and rules for buildings, CEN, Brussels; 2004.

[10] L. De Ceukelaire, D. Van Nieuwenburg, Accelerated carbonation of a blast-furnace cement concrete, Cem. Concr. Res. 23(2) (1993) 442-452.

[11] C. H. Malami, V. Kaloidas, G. Batis, N. Kouloumbi, Carbonation and porosity of mortar specimens with pozzolanic and hydraulic cement admixtures, Cem. Concr. Res. 24(8) (1994) 1444-1454.

[12] T. Sasatani, K. Torii, M. Kawamura, Five-year exposure test on long term properties of concretes containing fly ash, blast-furnace slag, and silica fume, *In: Proceedings of the 5th International Conference on the Use of Fly Ash, Silica Fume, Slag and Natural Pozzolans in Concrete*, ACI SP-153, Milwaukee, 1995, p. 283-296.

[13] V. G. Papadakis, Effect of supplementary cementing materials on concrete resistance against carbonation and chloride ingress, Cem. Concr. Res. 30(2) (2000) 291-299.

[14] C. D. Atiş, Accelerated carbonation and testing of concrete made with fly ash, Constr. Build. Mater. 17(3) (2003) 147-152.

[15] X. Zhang, K. Wu, A. Yan, Carbonation property of hardened binder pastes containing super-pulverized blast-furnace slag, Cem. Concr. Compos. 26(4) (2004) 317-374.

[16] J. Khunthongkeaw, S. Tangtermsirikul, T. Leelawat, A study on carbonation depth prediction for fly ash concrete, Constr. Build. Mater. 20(9) (2006) 744-753.

[17] K. Sisomphon, L. Franke, Carbonation rates of concretes containing high volume of pozzolanic materials, Cem. Concr. Res. 37(12) (2007) 1647-1653.

[18] D. O. McPolin, P. A. Basheer, A. E. Long, Carbonation and pH in mortars manufactured with supplementary cementitious materials, J. Mater. Civ. Eng. 21(5) (2009) 217-225.

[19] H. S. Shi, B. W. Xu, X. C. Zhou, Influence of mineral admixtures on compressive strength, gas

permeability and carbonation of high performance concrete, Constr. Build. Mater. 23(5) (2009) 1980-1985.

[20] Y. Gao, L. Cheng, Z. Gao, S. Guo, Effects of different mineral admixtures on carbonation resistance of lightweight aggregate concrete, Constr. Build. Mater. 43 (2013) 506-510.

[21] E. Gruyaert, P. Van den Heede, N. De Belie, Carbonation of slag concrete: effect of the cement replacement level and curing on the carbonation coefficient – effect of carbonation on the pore structure, Cem. Concr. Compos. 35(1) (2013) 39-48.

[22] A. Younsi, P. Turcry, A. Aït-Mokhtar, S. Staquet, Accelerated carbonation of concrete with high content of mineral additions: effect of interactions between hydration and drying, Cem. Concr. Res. 43 (2013) 25-33.

[23] S. D. Bahador, T. Y. Lim, S. Teng, Durability properties and microstructure of ground granulated blast furnace slag cement concrete, Int. J. Concr. Struct. Mater. 8(2) (2014) 157-164.

[24] A. Leeman, P. Nygaard, J. Kaufmann, R. Loser, Relation between carbonation resistance, mix design and exposure of mortar and concrete, Cem. Concr. Compos. 62 (2015) 33-43.

[25] A. Morandeau, M. Thiery, P. Dangla, Impact of accelerated carbonation on OPC cement paste blended with fly ash, Cem. Concr. Res. 67 (2015) 226-236.

[26] C.-Q. Lye, G.S. Ghataora, R.K. Dhir, Carbonation resistance of fly ash concrete, Mag. Concr. Res. 67(21) (2015) 1150-1178.

[27] C.-Q. Lye, G.S. Ghataora, R.K. Dhir, Carbonation resistance of GGBS concrete, Mag. Concr. Res. 68(18) (2016) 936-969.

[28] S. Boualleg, M. Bencheikh, L. Belagraa, A. Daoudi, M. A. Chikouche, The combined effect of the initial cure and the type of cement on the natural carbonation, the portlandite content, and nonevaporable water in blended cement, Adv. Mater. Sci. Eng. 2017 (2017) Article ID 5634713, 17 pages, https://doi.org/10.1155/2017/5634713.

[29] S. Miyahara, E. Owaki, M. Ogino, E. Sakai, Carbonation of a concrete using a large amount of blast furnace slag powder, J. Ceram. Soc. Jpn. 125(6) (2017) 533-538.

[30] R. Francois, J. C. Maso, Effect of damage in reinforced concrete on carbonation or chloride penetration, Cem. Concr. Res. 18(6) (1988) 961-970.

[31] A. Castel, R. Francois, G. Arliguie, Effect of loading on carbonation penetration in reinforced concrete elements, Cem. Concr. Res. 29(4) (1999) 561-565.

[32] C. Jiang, X. Gu, W. Zhang, W. Zou, Modeling of carbonation in tensile zone of plain concrete beams damaged by cyclic loading, Constr. Build. Mater. 77 (2015) 479-488.

[33] W. Wang, C. Lu, Y. Li, G. Yuan, Q. Li, Effects of stress and high temperature on the carbonation resistance of fly ash concrete, Constr. Build. Mater. 138 (2017) 486-495.

[34] X.-H. Wang, D. V. Val, L. Zheng, M. R. Jones, Influence of loading and cracks on carbonation of RC elements made of different concrete types, Constr. Build. Mater. 164 (2018) 12-28.

[35] S. Alahmad, A. Toumi, J. Verdier, R. Francois, Effect of crack opening on carbon dioxide penetration in cracked mortar samples, Mater. Struct. 42(5) (2009) 559-566.

[36] V. H. Dang, R. François, V. L'Hostis, D. Meinel, Propagation of corrosion in pre-cracked carbonated reinforced mortar, Mater. Struct. 48 (2015) 2575-2595.

[37] fib Bulletin 34, Model Code for Service-life Design, Lausanne: Switzerland; 2006.

[38] W. Ashraf, Carbonation of cement-based materials: Challenges and opportunities, Constr. Build. Mater. 120 (2016) 558-570.

[39] A. Silva, R. Neves, J. de Brito, Statistical modelling of carbonation in reinforced concrete, Cem. Concr. Compos. 50 (2014) 73-81.

[40] Earth's CO2 Home Page. https://www.co2.earth/ (accessed on August 14, 2018).

[41] EN 1990, Eurocode 0. Bases of structural design, CEN. Brussels; 2002.

[42] S. O. Ekolu, A review of effects of curing, sheltering, and CO_2 concentration upon natural carbonation of concrete, Constr. Build. Mater. 127 (2016) 306-320.

[43] M. G. Stewart, X. Wang, M. N. Nguyen, Climate change impact and risks of concrete infrastructure deterioration, Eng. Struct. 33(4) (2011) 1326-1337.

[44] Intergovernmental Panel on Climate Change (IPCC) Data Distribution Centre. http://www.ipcc-

data.org/observ/ddc_co2.html (accessed on August 14, 2018)

Appendix A

Table 1A Carbonation depths in concrete specimens subjected to 120-day accelerated carbonation.

Concrete type	Specimens		Average carbonation depth* (mm)				Maximum carbonation depth (mm)	
			Top	Ave.	Bottom	Ave.	Top	Bottom
040PC	Cube		0		0		-	-
	Beams	040PC01	0		0		0	0
		040PC03	3.5		6.3		17.2	17.8
055PC	Cube		18.9		16.1		-	-
	Beams	055PC01	14.3	14.3	18.8	17.9	25.5	43.5
		055PC03	14.3		16.9		24.7	38.9
040FA	Cube		19.3		18.5		-	-
	Beams	040FA01	17.0		20.8		23.3	59.7
		040FA03	17.9	16.1	24.4	21.6	30.6	52.0
		040FA03(2)	13.5		19.6		20.6	63.6
055FA	Cube		24.4		18.5		-	-
	Beams	055FA01	25.4	20.8	48.1	43.5	49.7	64.1
		055FA03	16.1		38.8		28.7	65.7
040GGBS	Cube		11.6		10.6		-	-
	Beam	040GGBS03	10.6		15.1		24.6	42.9
055GGBS	Cube		15.2		12.0		-	-
	Beams	055GGBS01	21.6	20.3	24.4	27.1	30.2	47.4
		055GGBS03	19.0		29.8		23.7	86.0

* Over the 200-mm long central segment excluding the influence of visible flexural cracks

Appendix B

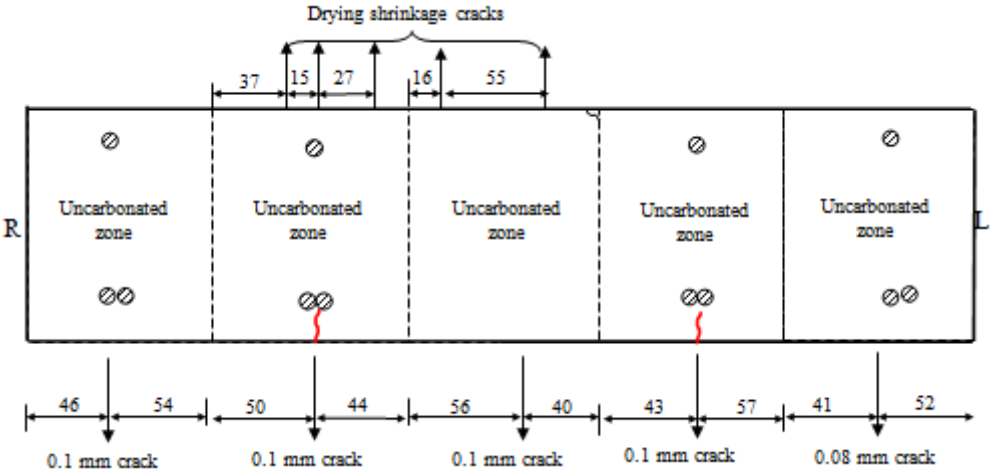

(a) 040PC01 (2)

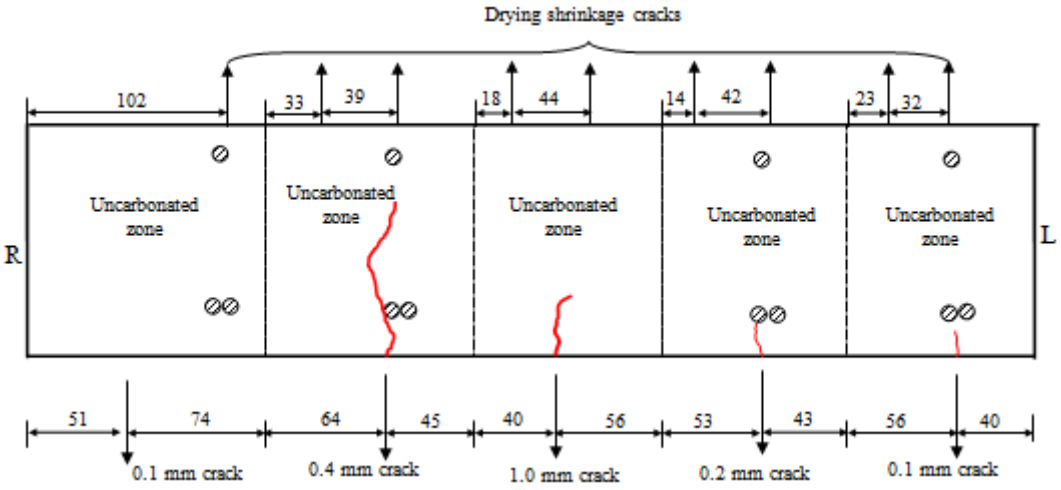

(b) 040PC03 (2)

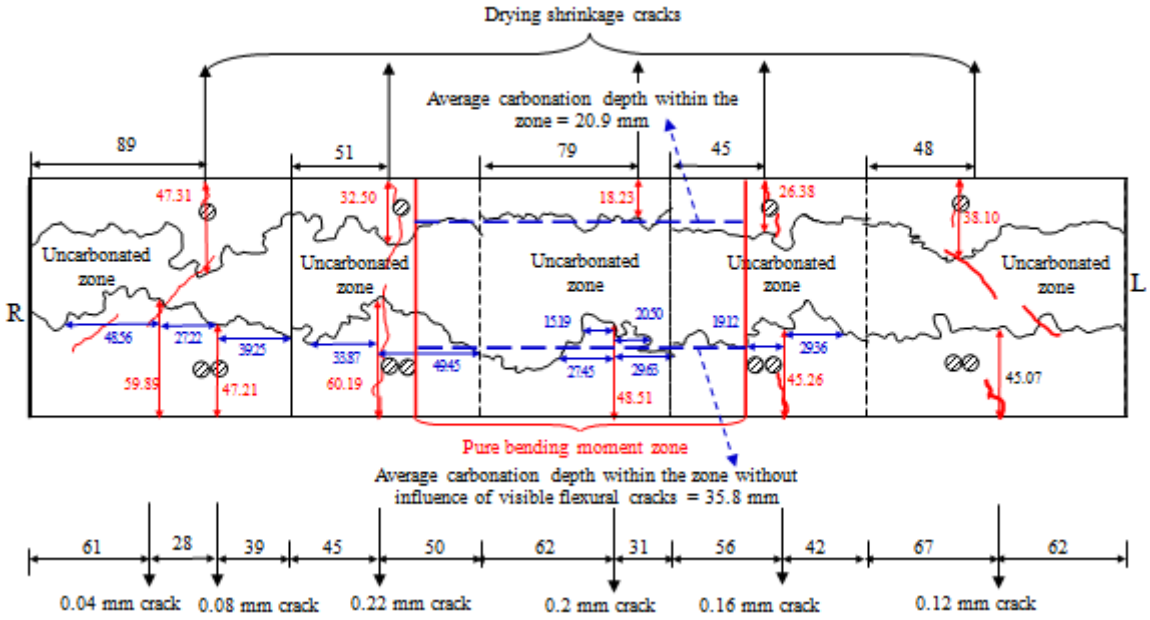

(c) 055PC01 (2)

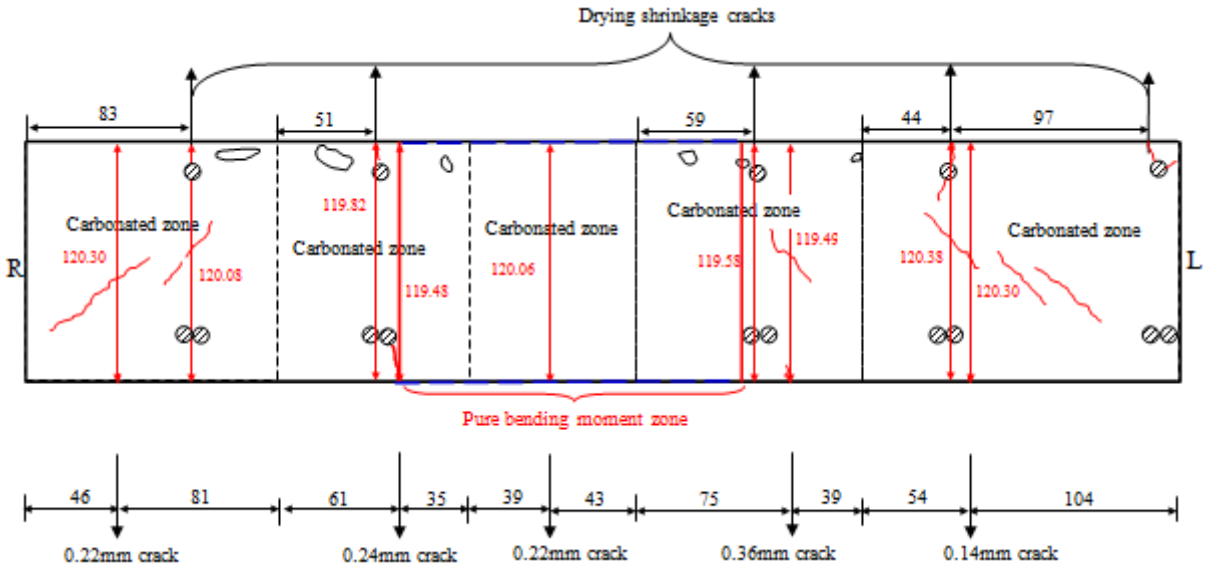

(d) 055FA01(2)

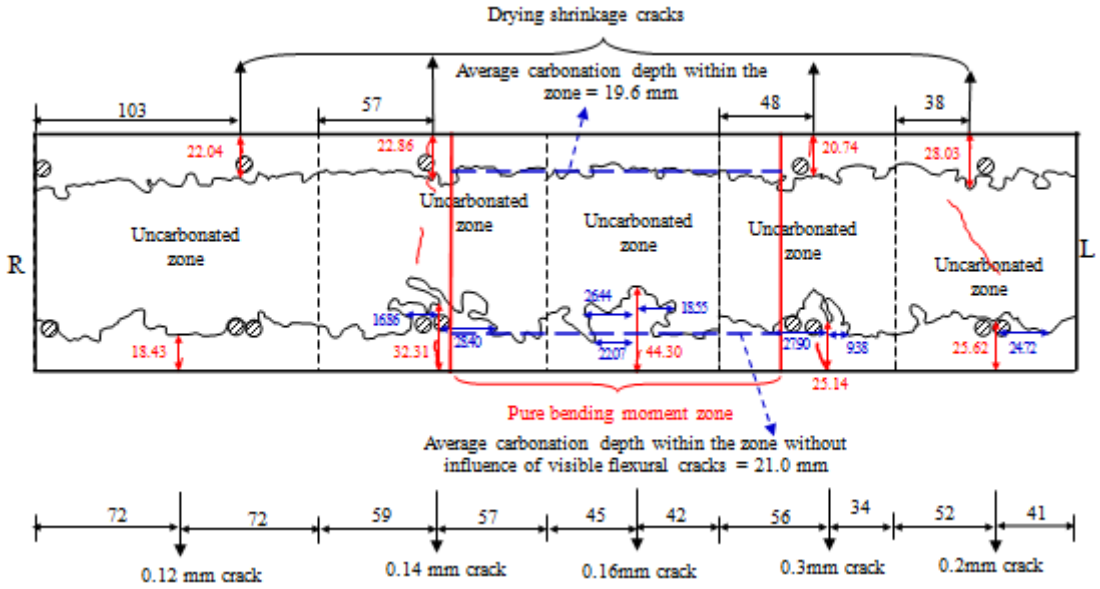

(e) 040GGBS01 (2)

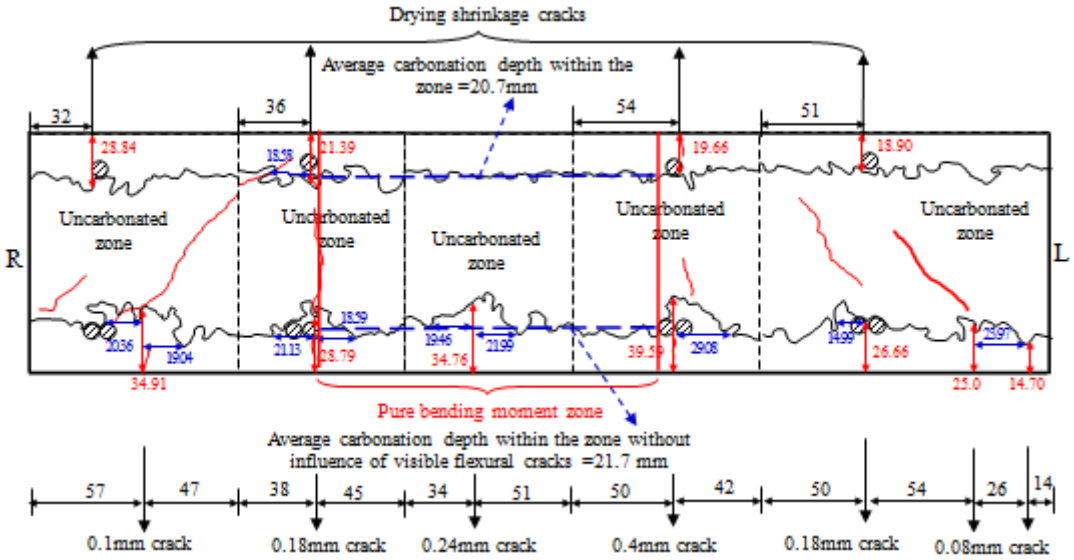

(f) 040GGBS03 (2-2)

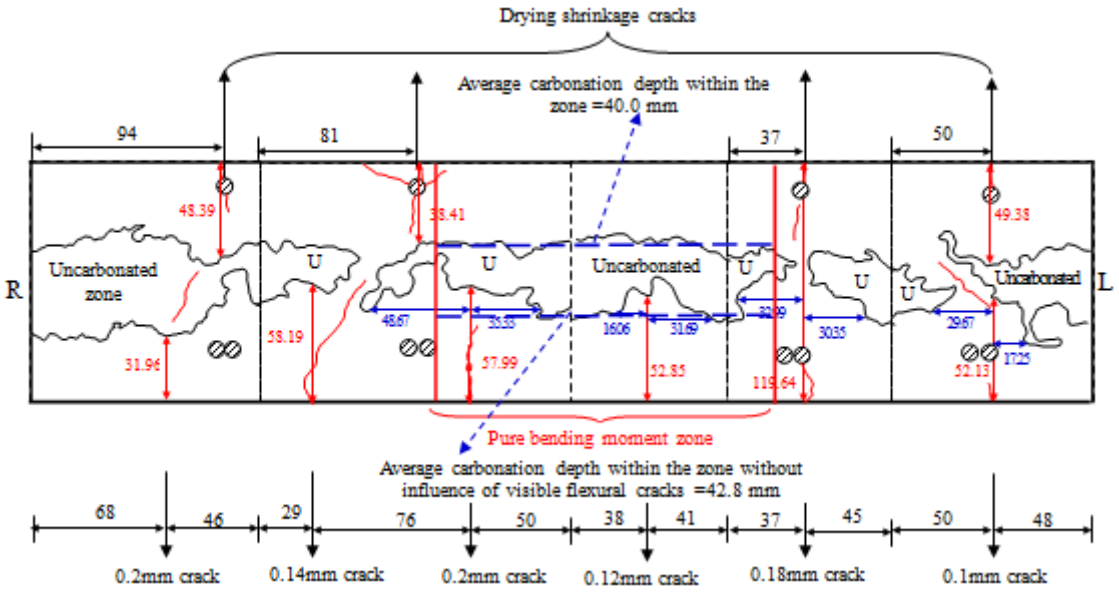

(g) 055GGBS01(2)

Fig. 1B Carbonation profiles of loaded beams of 040PC01(2), 040PC03(2), 055PC01(2), 055FA01(2), 040GGBS01(2), 040GGBS03(2-2) and 055GGBS01(2) after 120 days of carbonation.

List of figure captions

List of table captions

List of Figures

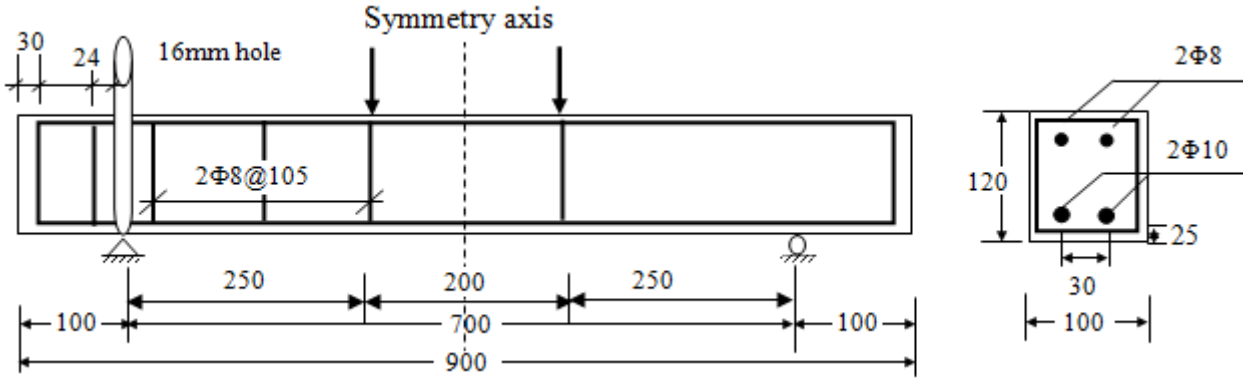

(a) Sketch of RC beam specimen [34].

(b) Cubes and the beam pairs kept in carbonation chamber for 240 days.

Fig.1 Sketch of RC beam specimen and photo of test specimens kept in the carbonation chamber.

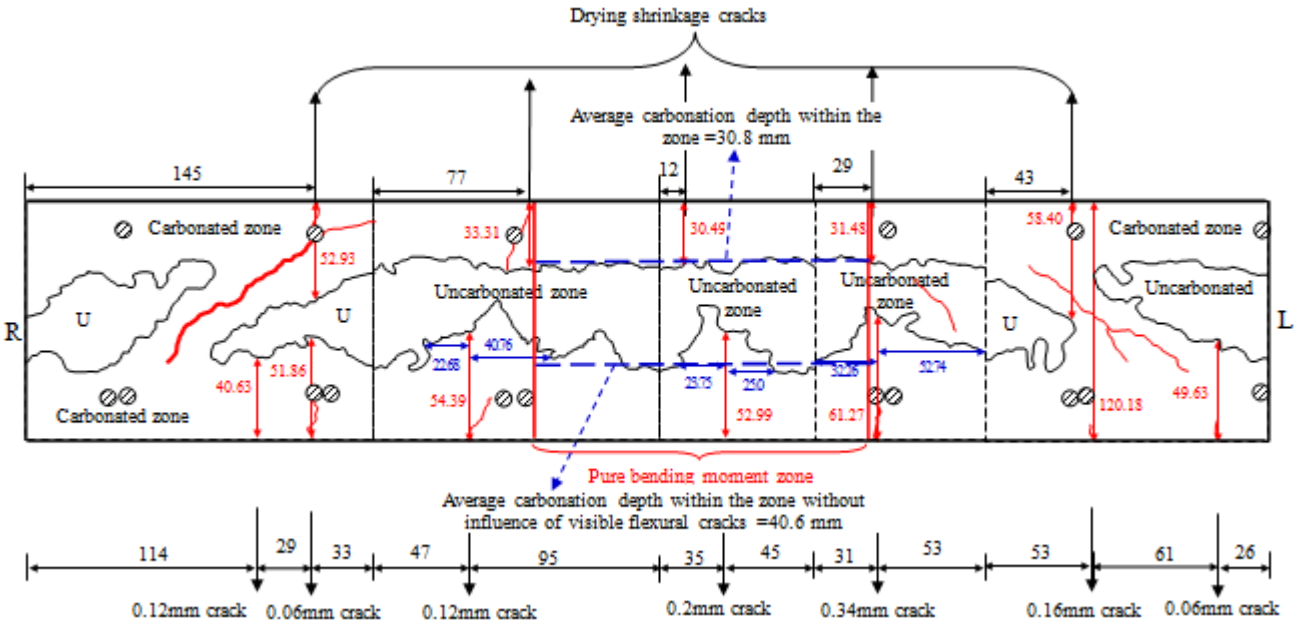

(a) 040FA03(2-2)

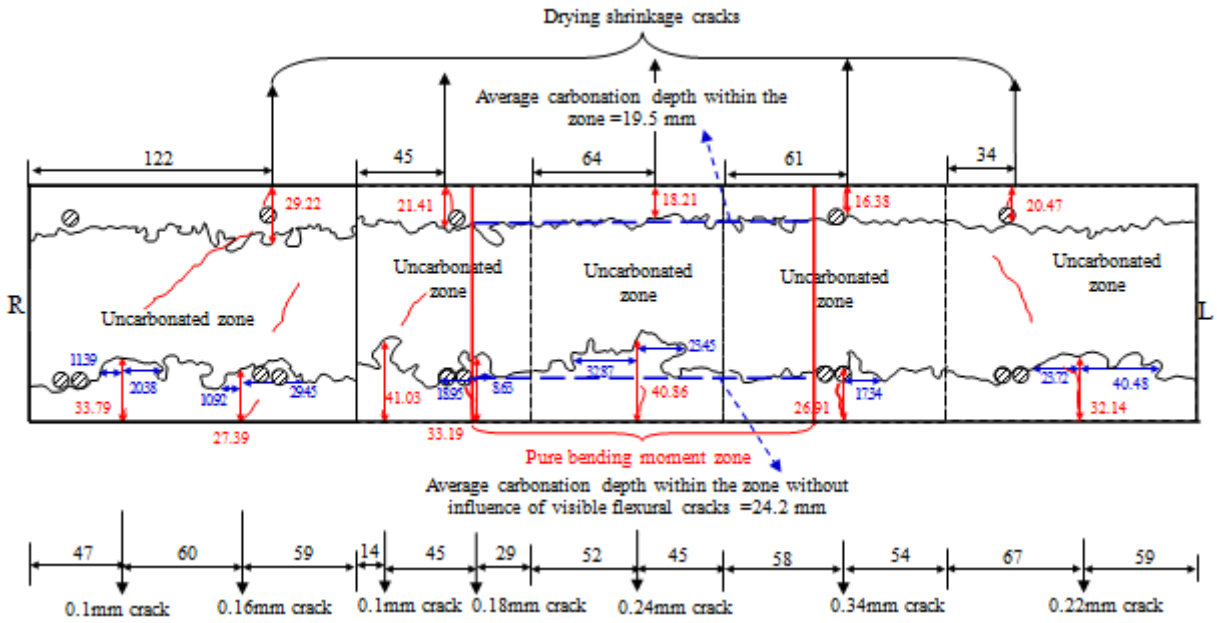

(b) 040GGBS03(2)

Fig.2 Comparison of carbonation profiles of typical loaded beams of 040FA and 040GGBS. Note: The measured carbonation profiles and visible crack are indicated by black lines and red lines, respectively; vertical carbonation depths at crack locations (i.e. flexural cracks at the bottom and drying shrinkage cracks at the top) are indicated by red numbers and red straight lines with arrows at both ends; while horizontal carbonation are indicated by blue numbers and blue straight lines with arrows at both ends.

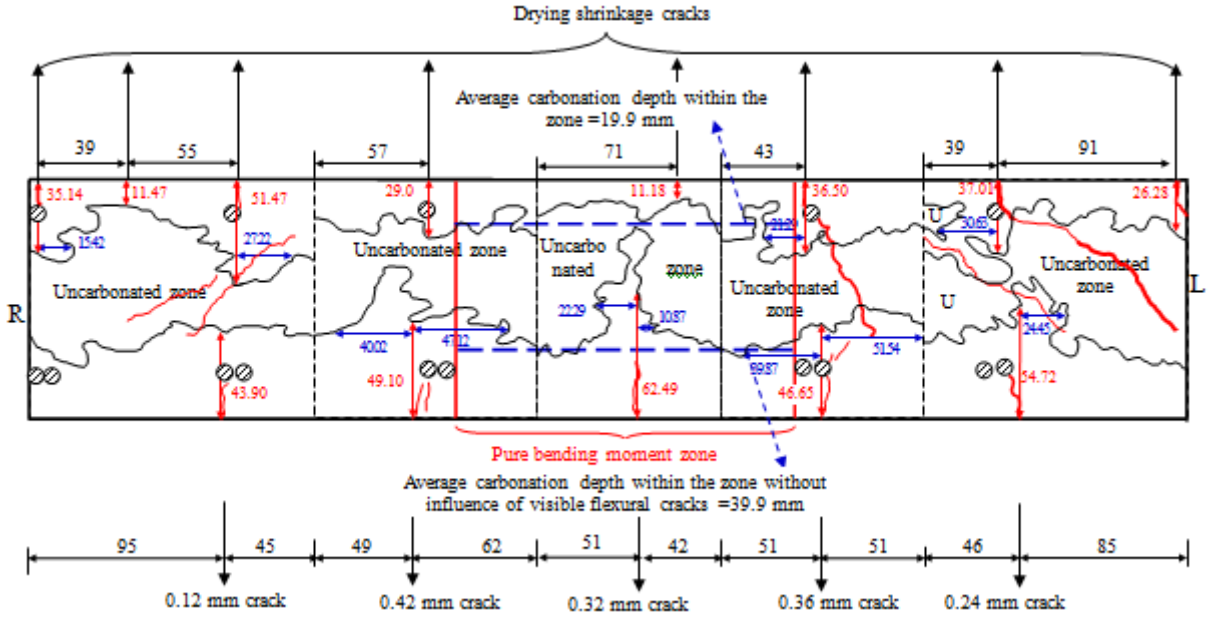

(a) 055PC03 (2)

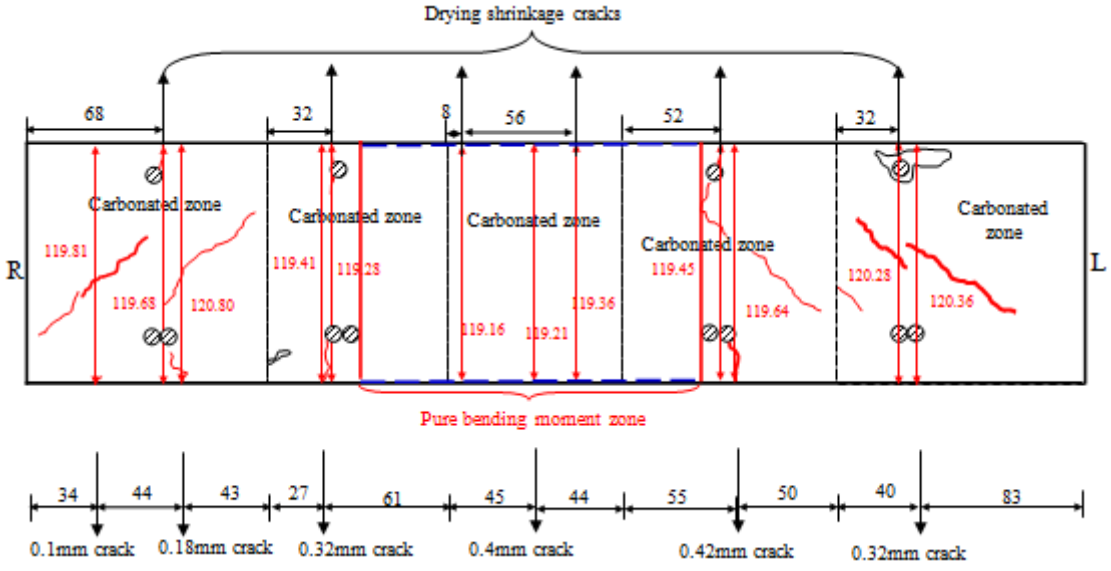

(b) 055FA03(2)

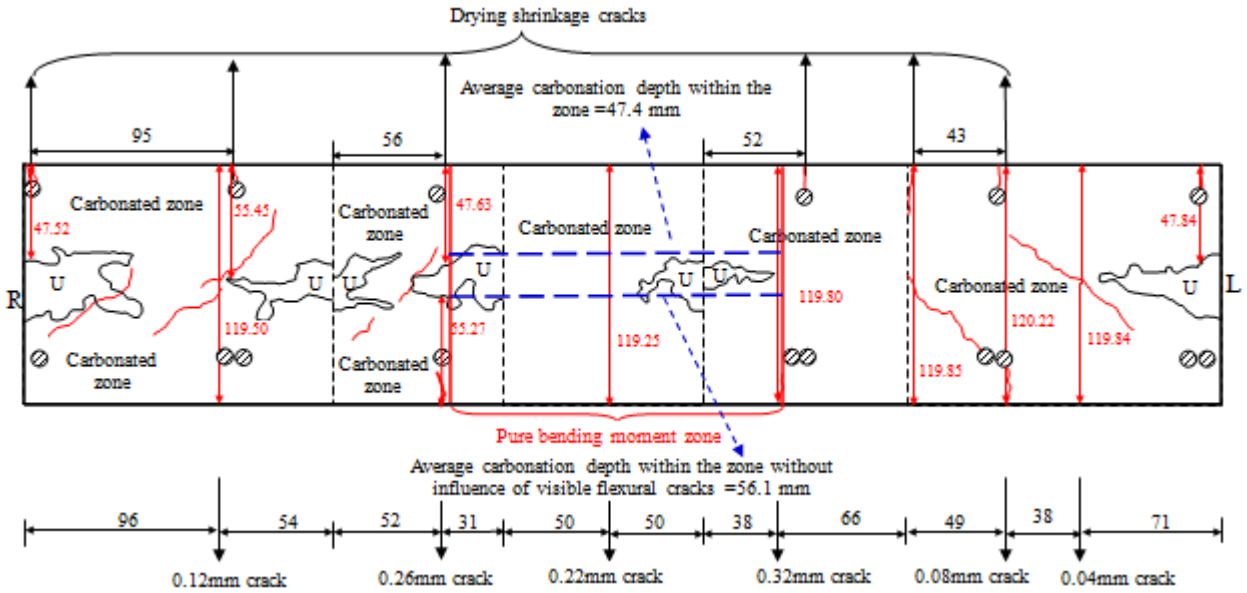

(c) 055GGBS03(2)

Fig.3 Comparison of carbonation profiles of typical loaded beams of 055PC, 055FA and 055GGBS.

Note: The measured carbonation profiles and visible crack are indicated by black lines and red lines, respectively; vertical carbonation depths at crack locations (i.e. flexural cracks at the bottom and drying shrinkage cracks at the top) are indicated by red numbers and red straight lines with arrows at both ends; while horizontal carbonation are indicated by blue numbers and blue straight lines with arrows at both ends.

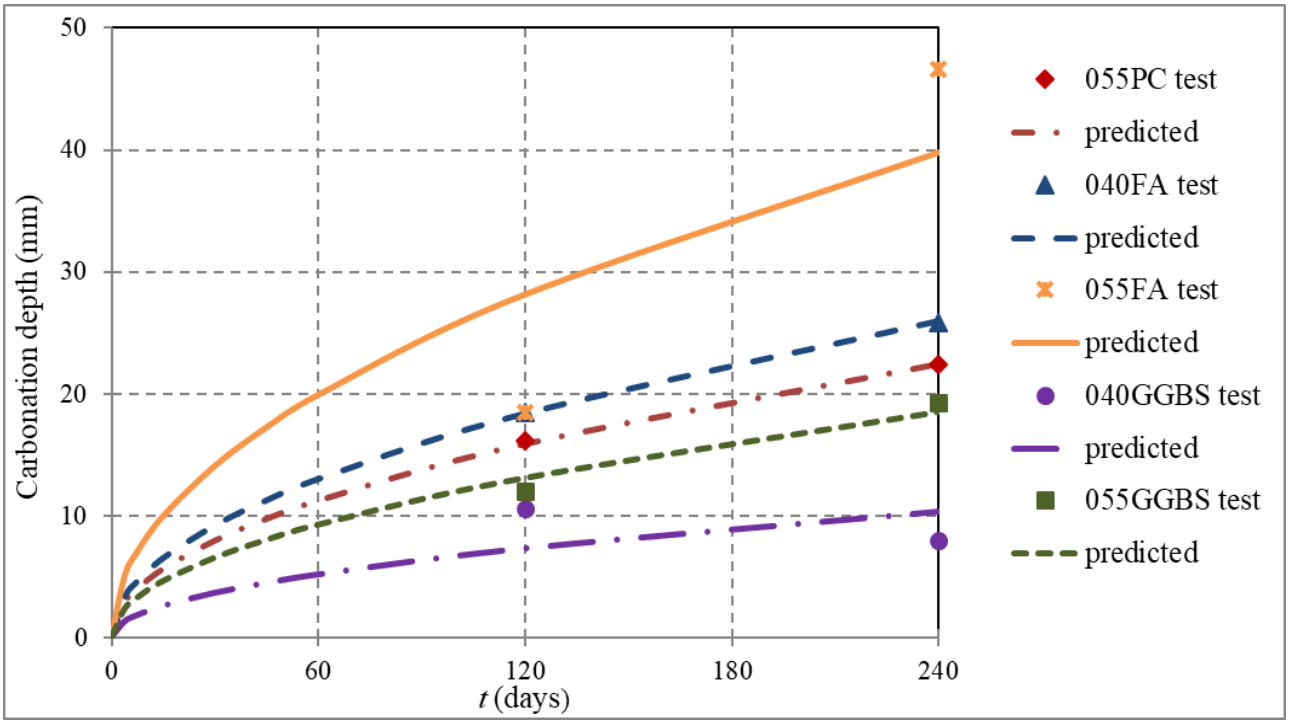

(a) Unloaded cubes

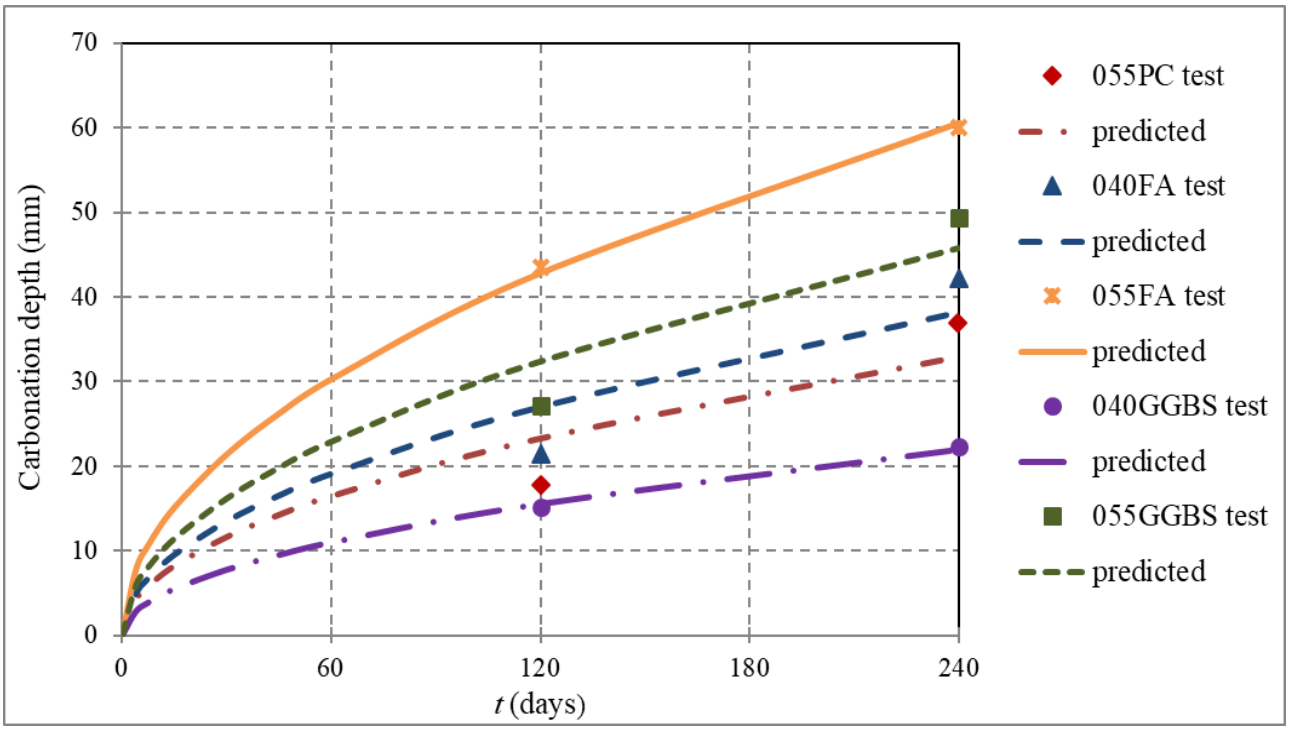

(b) Loaded beams

Fig.4. Average carbonations depths from the tests and fitted predictions.

List of Tables

Table 1 Details of RC beam specimens (stage two).

Test specimens	Cross section(mm)		Average clear concrete cover of 10-mm bars in tensile zone (mm)	Average clear concrete cover of stirrups		Maximum width of flexural cracks (mm)
	Width	Height		Tensile zone	Compression zone	
040PC01(2)	99.9	121.3	27.1	18.3	13.1	0.1
040PC03(2)	99.6	120.5	28.8	19.0	12.1	1.0
055PC01(2)	99.4	121.1	32.0	21.2	10.1	0.38
055PC03(2)	99.1	120.4	29.7	20.2	11.4	0.42
040FA03(2-2)	98.9	121.3	27.7	17.8	11.5	0.34
055FA01(2)	99.2	120.3	29.0	19.2	10.3	0.36
055FA03(2)	99.6	120.3	29.1	19.7	9.3	0.42
040GGBS01(2)	99.4	120.0	28.6	18.2	11.0	0.3
040GGBS03(2)	99.2	120.5	27.5	18.2	11.6	0.38
040GGBS03(2-2)	99.4	121.4	28.7	18.5	11.6	0.4
055GGBS01(2)	99.1	120.7	29.4	20.9	9.3	0.3
055GGBS03(2)	98.7	120.0	29.7	19.6	9.9	0.32

Note: beam test specimens were identified with concrete mix followed by two digits that define the maximum width of the initial flexural cracks and stage number (e.g. “040PC01(2)” is a PC concrete beam with a w/b ratio of 0.40 and the maximum initial crack width of 0.1 mm at the stage two) .

Table 2 Carbonation depths in concrete cubes and beam specimens subjected to 240-day accelerated carbonation.

Concrete type	Specimens		Average carbonation depth* (mm)				Maximum carbonation depth (mm)			
			Top	Ave.	Bottom	Ave.	Top	Ave.	Bottom	Ave.
040PC	Cube	040PC (1)	0	0	0	0	-		-	
		040PC (2)	0		0					
	Beams	040PC01(2)	0	0	0	0	0	0	0	0
			0		0		0		0	
		040PC03(2)	0	0	0	0	0	0	0	0
			0		0		0		0	
055PC	Cube	055PC (1)	27.5	28.4	21.8	22.4	-		-	
		055PC (2)	29.3		22.9					
	Beams	055PC01(2)	20.9	21.8	35.8	33.7	48.0	42.5	64.8	60.4
			22.7		31.5		37.0		56.0	
		055PC03(2)	19.9	19.6	39.9	39.9	51.5	53.0	97.5	94.8
			19.3		39.9		54.4		92.1	
040FA	Cube	040FA (1)	25.7	25.2	24.7	25.9	-		-	
		040FA (2)	24.7		27.0					
	Beam	040FA03(2-2)	30.8	31.3	40.6	42.2	Some zones are totally carbonated through whole beam height			
			31.8		43.7					
055FA	Cube	055FA (1)	Totally carbonated	47.4	Totally carbonated	46.7	-		-	
		055FA (2)	44.7		43.3					
	Beams	055FA01(2)	Totally carbonated through whole beam height							
			Totally carbonated through whole beam height							
		055FA03(2)	Totally carbonated through whole beam height							
			Totally carbonated through whole beam height							
040GGBS	Cube	040 GGBS (1)	9.3	10.3	9.2	8.0	-		-	
		040 GGBS (2)	11.3		6.7					
	Beams	040GGBS01(2)	19.6	20.1	21.0	21.0	28.7	29.6	44.3	43.0
			20.6		21.0		30.5		41.7	
		040GGBS03 (2)	19.5	19.5	24.2	24.4	29.4	30.0	45.9	43.0
			19.5		24.6		30.5		40.1	
		040GGBS03 (2-2)	20.7	19.8	21.7	21.6	29.3	29.4	40.1	39.8
			18.8		21.5		29.4		39.5	
055GGBS	Cube	055 GGBS (1)	22.6	23.0	16.4	19.3	-		-	
		055 GGBS (2)	23.4		22.1					
	Beams	055GGBS01(2)	40.0	39.6	42.8	42.5	Some zones are totally carbonated through whole beam height			
			39.1		42.2					
		055GGBS03(2)	47.4	47.5	56.1	56.3	Most zones are totally carbonated through whole beam height			
			47.5		56.4					

* Over the 200-mm long central segment excluding the influence of visible flexural cracks

Table 3 Density, absorption and void content of the different concretes [34].

Concrete mix	Concrete cubes						Results					
	Mass in air (g)			Mass in water* (g)	Volume (cm^3)		Density (kg/m3)			Absorption	Void content	
		As-received	Oven-dried	Water saturated			As-received	Oven-dried	Water saturated	(%)	(%)	Mean
040PC	1	2378.6	2317.4	2440.7	1379.8	994.3	2392.2	2330.7	2454.7	5.3	12.4	12.3
	2	2403.7	2343.1	2465.5	1396.6	1002.3	2398.2	2337.7	2459.8	5.2	12.2	
055PC	1	2288.2	2231.3	2383.6	1322.9	994.1	2301.8	2244.5	2397.7	6.8	15.3	15.2
	2	2301.2	2243.2	2393.5	1332.3	994.6	2313.7	2255.4	2406.5	6.7	15.1	
040FA	1	2352.7	2299.2	2430.7	1355.2	1008.9	2331.9	2278.9	2409.3	5.7	13.0	12.9
	2	2358.5	2308.5	2437.5	1362.6	1008.3	2339.1	2289.5	2417.4	5.6	12.8	
055FA	1	2298.3	2246.1	2402.0	1330.4	1005.0	2286.9	2234.9	2390.0	6.9	15.5	15.6
	2	2291.6	2238.2	2394.6	1325.2	1002.8	2285.2	2232.0	2387.9	7.0	15.6	
040GGBS	1	2403.2	2336.8	2458.9	1385.4	1006.9	2386.7	2320.8	2442.0	5.2	12.1	12.1
	2	2418.3	2351.9	2473.5	1393.2	1013.7	2385.6	2320.1	2440.1	5.2	12.0	
055GGBS	1	2347.6	2284.1	2429.8	1355.7	1007.5	2330.1	2267.1	2411.7	6.4	14.5	14.5
	2	2351.0	2281.8	2427.9	1353.5	1007.8	2332.8	2264.1	2409.1	6.4	14.5	

*The mass includes the mass of the stirrup (66.6 g) that supported the immersed concrete cube in water.

Table 4 Carbonation coefficients in unloaded and loaded (tension) concretes.

Concrete mix	Carbonation coefficient (mm/√day)		Ratio A_l/A_u
	Unloaded, A_u	Loaded, A_l	
040PC	-*	-*	-
055PC	1.45	2.13	1.47
040FA	1.68	2.47	1.47
055FA	2.57	3.90	1.52
040GGBS	0.66	1.42	2.15
055GGBS	1.19	2.95	2.48

* Insufficient experimental data to estimate this value of A

Table 5 Carbonation depths and concrete cover requirements (50-year design working life).

Concrete mix	Carbonation depth (mm)		Required minimum cover thickness (mm) [9]	
	Unloaded	Loaded	XC2/XC3	XC4
040PC	-*	-*	30	35
040FA	22.7	**33.4**		
040GGBS	9.0	19.2		
055PC	19.6	28.7	35	40
055FA	34.7	**52.7**		
055GGBS	16.1	**39.9**		

* Insufficient experimental data to estimate this carbonation depth

Table 6 Carbonation depths and concrete cover requirements (100-year design working life).

Concrete mix	Carbonation depth (mm)		Required minimum cover thickness (mm) [9]	
	Unloaded	Loaded	XC2/XC3	XC4
040PC	-*	-*	40	45
040FA	32.1	**47.2**		
040GGBS	12.6	27.1		
055PC	27.7	40.7	45	50
055FA	**49.1**	**74.5**		
055GGBS	22.7	**56.4**		

* Insufficient experimental data to estimate this carbonation depth